J. Phycol. **55,** 912–923 (2019)

DOI: 10.1111/jpy.12882

MOLECULAR PHYLOGENY AND EVOLUTION OF PHENOTYPE IN SILICA-SCALED CHRYSOPHYTE GENUS *MALLOMONAS*[1]

Dora Čertnerová[2]

Department of Botany, Faculty of Science, Charles University, Benátská 2, CZ-12800 Prague, Czech Republic
dora.certnerova@gmail.com

Martin Čertner

Department of Botany, Faculty of Science, Charles University, Benátská 2, CZ-12800 Prague, Czech Republic
Institute of Botany, The Czech Academy of Sciences, Zámek 1, CZ-25243 Průhonice, Czech Republic

and Pavel Škaloud

Department of Botany, Faculty of Science, Charles University, Benátská 2, CZ-12800 Prague, Czech Republic

The evolution of phenotypes is highly understudied in protists, due to the dearth of morphological characters, missing fossil record, and/or unresolved phylogeny in the majority of taxa. The chrysophyte genus *Mallomonas* (Stramenopiles) forms species-specific silica scales with extraordinary diversity of their ornamentation. In this paper, we molecularly characterized three additional species to provide an updated phylogeny of 43 species, and combined this with evaluations of 24 morphological traits. Using phylogenetic comparative methods, we evaluated phylogenetic signal in traits, reconstructed the trait evolution, and compared the overall phylogenetic and morphological diversity. The majority of traits showed strong phylogenetic signal and mostly dynamic evolution. Phylogenetic relatedness was often reflected by the phenotypic similarity. Both V-rib and dome are very conservative structures that are presumably involved in precise scale overlap and bristle attachment, respectively. Based on modern species, it seems the dome firstly appeared on apical and/or caudal scales, and only later emerged on body scales. Bristle was presumably present in the common ancestor and gradually elongated ever since. However, most other morphological traits readily changed during the evolution of *Mallomonas*.

Key index words: **bristle; Chrysophyceae; dome; *Mallomonas*; phenotypic evolution; phylogenetic comparative methods; phylogeny; silica scales; V-rib**

***Abbreviations*: BI, Bayesian inference; BIC, Bayesian information criterion; dNTP, deoxynucleoside triphosphate; Ma, million years ago; MES, 2-(N-morpholino)ethanesulfonic acid; ML, maximum likelihood; PCoA, principal coordinates analysis; PGLS, phylogenetic generalized least squares; PP, posterior probabilities; wMP, weighted maximum parsimony**

The shape diversity in modern living forms is usually a result of various evolutionary processes. Many factors can influence the evolvement of organismal body plan (e.g., adaptation, neutral evolution, or non-adaptive factors like spandrels or constraints; Darwin 1859, Gould 2002, Nei 2005, Orr 2005, Brakefield and Roskam 2006). The phenotype of organisms can change either rapidly, especially when associated with a speciation event (i.e., punctuated evolution; Eldredge and Gould 1972), gradually (i.e., gradual evolution; Darwin 1859), or stay unmodified for a long time in so called evolutionary stasis (Gersick 1991). Although the latter may seem like a passive state, the phenotype needs to remain unchanged in spite of selection pressures and/or fluctuations caused by stochastic processes (Erwin 2000).

Morphological evolutionary changes usually take place over long time periods and thus cannot be studied directly. One possibility is to study a fossil record; however, that brings a lot of complications (e.g., fragmentation of the fossil record or rareness of fossilization in a majority of taxa; Eldredge and Gould 1996). A convenient alternative is to apply phylogenetic comparative approaches to track the evolution of phenotypes based on modern species. The modern phylogenetic comparative biology combines the relationships between taxa with morphological data to model statistical inferences about their evolutionary past (Revell 2013). By using these approaches, we can reconstruct the past forms of traits in extinct ancestral taxa inferred from the trait values in their modern descendants (Schluter et al. 1997).

Unfortunately, it is extremely difficult to study phenotypic evolution in protists, considering the

[1]Received 5 November 2018. Accepted 5 April 2019. First Published Online 4 May 2019. Published Online 24 June 2019, Wiley Online Library (wileyonlinelibrary.com).
[2]Author for correspondence: e-mail dora.certnerova@gmail.com.
Editorial Responsibility: O. De Clerck (Associate Editor)

dearth of easily scorable traits, frequently spherical shape of their bodies, and poorly resolved phylogenetic relationships in the majority of lineages. Moreover, a lack of structures that could be preserved in sediment leads to a very limited fossil record in protists, which also constrains the proper calibration of phylogenetic analyses (Roger and Hug 2006). Nevertheless, some protist lineages are able to produce minerals preserved in fossil layers by a process of biomineralization (e.g., Bovee 1981, Henriksen et al. 1993, Mayama and Kuriyama 2002, Morais et al. 2017). The most well-known protists forming mineral structures are diatoms (Martin-Jezequel et al. 2000); though, several other clades in Stramenopiles are capable of creating extraordinarily diverse biomineralized structures. Probably, the most prominent are the structures formed by several representatives of the class Chrysophyceae, including its largest genus, *Mallomonas* (Kristiansen 2002). The genus *Mallomonas* comprises unicellular autotrophic flagellates, commonly found in plankton of freshwater lakes and ponds. These organisms form scales, cysts, and bristles made of silicon dioxide (Kristiansen 2005, Siver 2013). The basic scale design is a flat plate with posterior upturned rim, commonly perforated by small pores. However, scales are usually much more complex, complemented with papillae, ribs, or reticulations (Fig. 1). One of the most prominent structures that can be found on scales is a V-shaped rib called V-rib. This structure helps scales to overlap on a cell surface to create a highly organized and compact silica case (Siver and Glew 1990, Lavau and Wetherbee 1994, Siver et al. 2015). The end of the V-rib is often prolonged into two additional ribs, named anterior submarginal ribs. They usually link the V-rib with a dome, another prominent scale structure. The dome is a convex proximal part of scale that is usually involved in bristle attachments (Siver 1991).

Based on the scale position on a cell surface, we can recognize caudal, apical, and body scales with their specific shapes and features. Most parts of the cell are covered by body scales. The scales exhibit an extraordinary phenotypic diversity, but their shape remains species-specific and is typically used for species determination (Kristiansen 2005). The silica scales can be preserved in sediment for millions of years (Siver et al. 2015). Currently, there are two major localities with massive assemblages of fossil *Mallomonas* siliceous structures, Wombat and Giraffe, dating back to Paleocene and Middle Eocene, respectively. Aside from extinct taxa, fossilized siliceous scales with clear similarities to contemporary species have been recorded there (e.g., Siver and Wolfe 2005, 2009, Siver et al. 2013a, Wolfe and Siver 2013).

A number of studies focusing on the phylogeny of the genus *Mallomonas* have been published (Lavau et al. 1997, Andersen 2007, Jo et al. 2011, 2013, Škaloud et al. 2013a, Kim et al. 2014, Siver et al. 2015). Jo et al. (2011) were the first who suggested that two *Mallomonas* subclades (described later as A1 and A2 by Siver et al. 2015) can be distinguished by the presence or absence of the V-rib. In addition, Jo et al. (2011) estimated the origin of the genus in the Early Jurassic, approximately at 150 Ma, and the divergence between the two subclades in the Early Cretaceous, approximately at 133 Ma. The period of origin and the divergence estimations made by Siver et al. (2015) were slightly younger, dated in the Early Cretaceous, at ~135 and 113 Ma, respectively. According to Siver et al. (2015), the earliest-diverging taxa are *M. insignis* within A1 subclade and three closely related species, *M. bangladeshica*, *M. peronoides*, and *M. ceylanica* within A2 subclade. All these taxa have very complex scales with reticulation, papillae, or a U-shaped ridge, which contradicts an early assumption that scales with basal morphology lacking any additional structures are the most ancient ones (Asmund and Kristiansen 1986, Kristiansen 2002). This stresses the need for better understanding of the morphological evolution of scales in the genus *Mallomonas*. However, our knowledge of the phylogenetic relationships between the *Mallomonas* taxa is still limited. Primarily due to the considerable dearth of *Mallomonas* spp. cultures (probably caused by difficulties with their cultivation), only 18% of currently

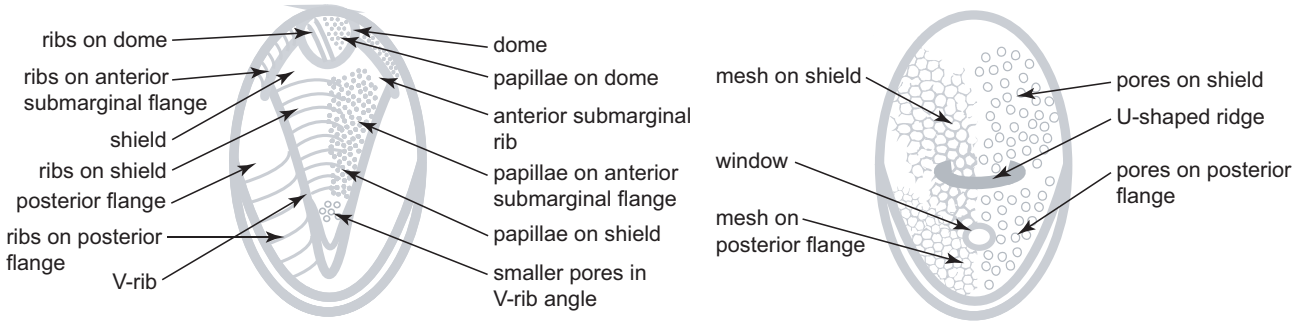

FIG. 1. Schematic depiction of siliceous body scales of *Mallomonas* showing the main morphological features of their ornamentation that were evaluated for the reconstruction of shape evolution in the genus.

recognized species were molecularly characterized prior to this research. The main aim of this study was to provide an updated time-calibrated phylogeny of the genus *Mallomonas* supplemented with newly sequenced taxa, and to study in detail the evolution of phenotype by using phylogenetic comparative methods.

MATERIALS AND METHODS

Origin and cultivation of the investigated strains. New isolates of the genus *Mallomonas* were obtained from plankton and metaphyton samples collected in water bodies across Europe using a plankton net (mesh size of 20 μm). Collection details, strain information, and sequence accession numbers are listed in Table S1 in the Supporting Information. The cells were isolated using a sterile Pasteur capillary pipette, and brought into single-cell culture. The isolates were grown in 400 μL of either MES- or HEPES-buffered DY IV medium (Andersen et al. 1997) at 14°C (cooling box Pol-Eko Aparatura Sp.J., model ST 1 Wodzisław Śląski, Poland) under illumination of 35 μmol photons $\cdot$ $m^{-2} \cdot s^{-1}$ and 24 h light mode (TLD 18W/33 fluorescent lamps; Philips, Amsterdam, The Netherlands). As soon as cultures reached mid-exponential phase, 200 μL of each was harvested for molecular analyses.

Molecular analyses. After centrifugation, genomic DNA was extracted from the pellet of cells by InstaGene Matrix (Bio-Rad, Hercules, CA, USA). Two nuclear genes and one plastid gene were amplified (SSU rDNA, LSU rDNA, and *rbc*L, respectively). For the nuclear SSU rDNA, 18S-F and 18S-R primers were used (Katana et al. 2001). When amplifying the nuclear LSU rDNA region, we employed primers 28S_25F, 28S_1228F, 28S_861R and 28S_2160R (Jo et al. 2011), 28S_736F2 and 28S_1435R (Pusztai et al. 2016), and also a primer 28S_2022F (5′-ACT CAG AAC TGG AGC GGA CAA-3′) designed for this study using the Primer3 software (Untergasser et al. 2012). The plastid *rbc*L was amplified using rbcL_2F (Daugbjerg and Andersen 1997) and rbcL_R3 (Jo et al. 2011) primers.

Amplifications were performed in a total volume of 20 μL. For the nuclear SSU rDNA, PCR mix contained 0.2 μL of Gold DNA polymerase (Applied Biosystems, Foster City, CA, USA), 0.4 μL of dNTP, 2 μL of Gold Buffer (Applied Biosystems), 0.25 μL of each primer, 13.1 μL of double-distilled water, 2.2 μL of $MgCl_2$, 0.6 μL of enhancer (Applied Biosystems) and 1 μL of template DNA (not quantified). The amplification of nuclear LSU rDNA and plastid *rbc*L regions were performed in a PCR mix containing 0.2 μL of MyTaq HS DNA polymerase (Bioline, Taunton, MA, USA), 4 μL of MyTaqHS Buffer (Bioline), 0.4 μL of each primer, 14 μL of double-distilled water, and 1 μL of template DNA (not quantified). The amplifications were performed in Eppendorf Mastercycler ep Gradient 5341 (Eppendorf GmbH, Hamburk, Germany) using the following programs: 5 min of denaturation at 94°C for all gene regions; followed by 35 cycles of denaturation at 94°C (30 s to 1 min), annealing at 52°C/40°C/38°C for nuclear SSU and LSU rDNA and plastid *rbc*L region, respectively (1 min), and elongation at 72°C (2 min/4 min/2.5 min for nuclear SSU and LSU rDNA and *rbc*L region, respectively); with a final extension at 72°C (10 min), subsequently held at 10°C. The PCR products were sized on a 1% agarose gel and then purified using either GenElute PCR Clean-Up Kit (Sigma-Aldrich, St. Louis, MO, USA) or QIAEX II Gel Purification Kit (Qiagen, Chatsworth, CA, USA). The purified DNA templates were sequenced by Sanger Sequencing method at Macrogen, Inc. (Seoul, Korea, http://dna.macrogen.com). Newly obtained sequences were supplemented with GenBank-extracted sequences for 37 *Mallomonas* species, 30 representatives of related genera and two outgroup taxa (see Table S1). The alignment was automatically edited using Q-INS-i algorithm in MAFFT, ver. 7 (Katoh and Standley 2013) and then manually edited using MEGA 5 (Tamura et al. 2011). To improve the alignment quality, positions with deletions frequently occurring over the majority of sequences were removed. The resulting data set comprised of 1,712, 2,620, and 946 nucleotide sites for nuclear SSU rDNA, nuclear LSU rDNA and plastid *rbc*L regions, respectively.

Phylogenetic analyses. The data set was analyzed using Bayesian inference (BI) method implemented in Beast ver. 1.8.1. (Drummond and Rambaut 2007) to construct phylogeny and simultaneously estimate branch divergence times. To determine the best model for each molecular region, we used the Bayesian information criterion (BIC) in a likelihood-ratio test performed in jModeltest ver. 2.1.10 (Darriba et al. 2012). The GTR + G + I nucleotide substitution model was selected as the best model for all three molecular regions. Bayesian analysis with relaxed clock model and uncorrelated lognormal model was used to estimate variation rates across all branches. We used fossil calibrations as probabilistic priors. The lognormal priors were used for splits between the species *Mallomonas bangladeshica - M. peronoides*, *M. cratis - M. pseudocratis*, and *M. elevata - M. mangofera* var. *foveata*; and for the ancestors of species *Synura americana - S. conopea - S. glabra - S. macracantha - S. petersenii - S. truttae*, *Synura curtispina - S. mollispina - S. spinosa*, and *Chrysosphaerella brevispina - C. longispina - C. rotundata*. All calibrations were based on the following setting: offset = 38 Ma, mean = 30 Ma, and standard deviation = 0.6 Ma; representing a minimal age estimate for the majority of fossils of *Mallomonas* species from the Giraffe Pipe locality (Creaser et al. 2004, Doria et al. 2011). A Yule tree prior was used as a speciation model. The analysis ran for 100 million generations with chain sampling every 1,000 generations. The parameters-estimated convergence and burn-in period were checked using the software Tracer ver. 1.6. (Drummond and Rambaut 2007). The initial 1,500,000 trees (15%) were removed, the rest retained to construct a final chronogram with 95% posterior probabilities (PP) and age estimates for all nodes. The robustness of tree topologies was assessed by bootstrapping the data set with maximum-likelihood analysis (ML) and with weighted maximum parsimony analysis (wMP). The ML bootstrapping was performed by a heuristic search with 1,000 random sequence addition replicates and stepwise addition, using a Tree Bisection Reconnection branch-swapping algorithm using the program GARLI ver. 0.951 (Zwickl 2006). The wMP bootstrapping was performed using heuristic searches with 100 random sequences (the upper limit of 10,000 for each replicate) and gap characters were treated as the fifth character state using the program PAUP ver. 4.0 (Swofford 2001). Character weights were assigned using the rescaled consistency index on a scale of 0–1,000. New weights were based on the mean fit values for each character over all trees in the memory. Trees were visualized using FigTree ver.1.4.2. (Rambaut 2009).

Morphological analyses. Scales, bristles, and entire cell cases of cultured and sequenced *Mallomonas* strains were photographed using a transmission electron microscope (TEM) Jeol 1011 with integrated CCD camera Velvet (Olympus Soft Imaging Solution GmbH, Münster, Germany). The cysts were not included in this study because the majority of *Mallomonas* species has unknown cyst morphology (Kristiansen and Preisig 2007). For the 37 *Mallomonas* species with known molecular sequence data, we acquired TEM or scanning electron microscope (SEM) microphotographs from original descriptions and/or from the European chrysophyte database (Škaloud et al. 2013b). To evaluate phenotypes of the entire

set of 43 *Mallomonas* species used in this study, we scored 24 morphological traits on body scales, three traits on bristles, and two traits on silica cases (Table S2 in the Supporting Information). The trait values were either directly assessed from microphotographs, estimated by image analysis in ImageJ ver. 1.45s (Schneider et al. 2012) or alternatively taken from original descriptions (i.e., scale length and width, case length and width, bristle length). Trait estimates were averaged over multiple measurements of several silica scales (mean = 5, range 2–10) except for five species with only a single scale image available (*M. hexareticulata*, *M. lacuna*, *M. pseudomatvienkoae*, *M. sorohexareticulata*, and *M. splendens*). Morphological traits were examined for correlation using the Spearman correlation coefficient in R ver. 3.4.3 (R Development Core Team 2017). Since no pair of traits with absolute values of the coefficient >0.9 was detected, we retained all traits in the data set. Due to the fact that the number of measured traits exceeded the number of studied species, we used a principal coordinates analysis (PCoA) to visualize phenotypic differences among *Mallomonas* species. Trait values were standardized prior to analysis and the Gower coefficient was used for computing a similarity matrix to account for the presence of both binary and quantitative traits using software Canoco ver. 5 (Lepš and Šmilauer 2014).

Phylogenetic influence in traits. The phylogenetic influence was estimated using two scaling parameters, λ (lambda; Pagel 1999) and D (Fritz and Purvis 2010), on a reduced data set comprising of only *Mallomonas* representatives. The estimates were done in R using tools available in the library caper ver. 0.5.2 on data sets consisting of morphological trait values and tree topology. The scaling parameter λ was calculated to evaluate phylogenetic influence of quantitative traits using the phylogenetic generalized least squares (PGLS) method fitted by ML (Table S3 in the Supporting Information). Prior to the analysis, all the traits were natural log transformed, with exception of scale roundness with values ranging from 0 to 1. In PGLS of a given trait, only one parameter value was calculated at a time, and values of the remaining parameters were fixed to one. To evaluate phylogenetic influence for binary traits, the scaling parameter D was calculated in a Fritz-Purvis test with 10,000 permutations.

Mapping trait evolution on the phylogeny. The ancestral trait values at internal nodes were estimated based on the logarithmically transformed quantitative morphological trait values and the phylogenetic position of *Mallomonas* species using the contMap function implemented in R library phytools ver. 0.4-45 (Revell 2012). The quantitative ancestral character states were mapped onto the phylogenetic tree constructed by the ML method, using the Brownian motion function implemented in the ape library (Popescu et al. 2012). The ancestral characters with values interpolated along the branches of the tree were graphically visualized by Felsenstein's equation (Felsenstein 1985) using the contMap function. Evolution of binary traits was reconstructed by simulations with 999 repeats using make.simmap and dentistyMap functions in phytools.

After the PCoA was made on the entire morphological data set in Canoco ver. 5 (Lepš and Šmilauer 2014), we projected phylogenetic relationships among *Mallomonas* species into the PCoA ordination space to create a phylomorphospace plot using the phylomorphospace function in phytools.

RESULTS

Phylogenetic relationships among taxa. Time-calibrated phylogenetic analyses estimated the period of origin and phylogenetic position of taxa within Synurales (Fig. 2). According to our estimations, the genus *Neotessella* split between the Late Triassic and Early Cretaceous (213–124 Ma), most likely in the Late Jurassic at 163 Ma. The genera *Synura* and *Mallomonas* divided between the Middle Jurassic and Early Cretaceous (173–130 Ma), most probably in the Early Cretaceous at 135 Ma. About 20 million years after, the genus *Mallomonas* split into two major subclades A1 and A2 (sensu Siver et al. 2015) between the Early and Late Cretaceous (143–87 Ma), approximately in the Early Cretaceous at 113 Ma. We can distinguish the representatives of A1 and A2 subclades by the presence or absence of the V-rib on their body scales, with an exception of two taxa, *M. akrokomos* and *M. punctifera*. Phylogenetic position of three taxa, *M. intermedia*, *M. paludosa*, and *M. pumilio* var. *dispersa* was established for the first time. *Mallomonas intermedia* was inferred as a member of section *Mallomonas*, closely related to *M. portae-ferreae*, *M. corymbosa*, and *M. tonsurata*. *Mallomonas pumilio* var. *dispersa* was inferred as a member of the section *Torquatae*, sister to *M. torquata*. Interestingly, *M. paludosa*, originally described as a member of the section *Leboimeanae*, was with high statistical support nested within the section *Mallomonas*, closely related to the taxa *M. acaroides*, *M. crassisquama*, *M. morrisonensis*, and *M. muskokana*.

Reconstructions of trait evolution. Based on D and λ parameter indices, we detected a strong phylogenetic signal in 10 analyzed traits, specifically in the U-shaped ridge, bristle absence, bristle length, mesh on posterior flange, V-rib presence, V-rib angle, dome presence, dome size, scale area, and absolute proximal border width (Table S3).

A phylomorphospace plot combining the PCoA ordination plot of *Mallomonas* phenotypes with phylogenetic information indicated that closely related species generally have similar overall phenotypes (Fig. 3). Nonetheless, there are clearly several exceptions, for example, *M. adamas*, *M. akrokomos*, *M. heterospina*, *M. insignis*, and *M. punctifera*. While representatives of the sections *Quadratae*, *Planae*, *Insignes*, and *Punctiferae* are overlapping in their morphology, the section *Mallomonas* forms a well-delimited group based on both morphology and phylogeny (Fig. 3).

The reconstructed evolution of particular traits often displayed very different patterns (Figs. 4 and 5; Figs. S1 and S2 in the Supporting Information). Evolutionary trends observed in binary traits could be described by four scenarios. First, a structure was absent in the common ancestor of the genus and evolved once as a synapomorphy of a specific lineage (though may have later disappeared in some taxa). This is likely the case of two traits, mesh on posterior flange and U-shaped ridge (Fig. S1). Second, a structure was again absent in the common ancestor of the genus but evolved multiple times (again with secondary disappearance in some lineages). The evolution of most traits follows this scenario, for example absence of bristles, bristles

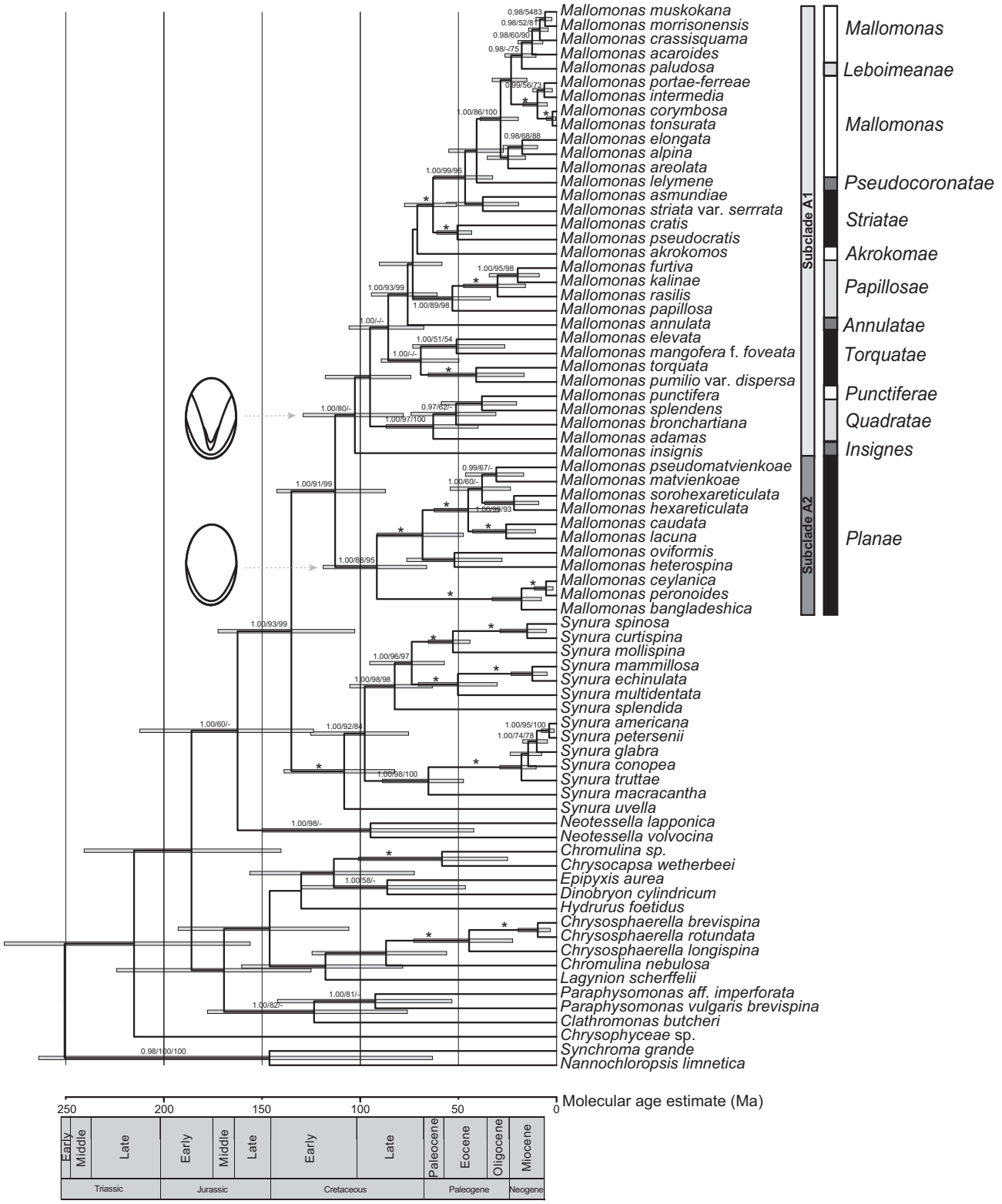

FIG. 2. Time-calibrated phylogenetic tree of the Chrysophyceae from a BEAST analysis. Values at nodes indicate statistical support estimated by three methods – Bayesian posterior probability (left), maximum-likelihood bootstrap (middle), and maximum parsimony bootstrap (right). An asterisk marks nodes with the highest statistical support (1.00/100/100). Grey error bars represent the 95% confidence intervals. The genus *Mallomonas* is divided in two subclades, A1 and A2, that differ by the presence or absence of a V-rib, respectively.

restricted to ends of cells, dome, papillae on anterior flange, papillae on dome, ribs on anterior and posterior flange, ribs on dome as well as smaller pores in V-rib angle (Fig. 4, Fig. S1). Third, the common ancestor possessed a structure which then disappeared in some lineages (i.e., papillae on shield, pores on shield and pores on posterior flange; Fig. 5, Fig. S1). Finally, the structure may not show any clear evolutionary trend (i.e., anterior submarginal rib, mesh on shield, V-rib and window; Fig. 4, Fig. S1).

In the case of quantitative traits, the evolutionary change (i.e., increase or decrease in trait values) may either follow general trends in the whole genus, or, alternatively, be species- or lineage-specific. A general evolutionary trend can be observed only in a single trait, bristle length, which seems to gradually increase during the evolution of the genus *Mallomonas* (Fig. 4). However, evolution of the remaining traits is consistent with the second scenario of lineage-specific trends (Fig. 5, Fig. S2). When comparing the reconstructed evolution of two related traits, we might see different effects on the overall phenotype. For instance, proportional increase/decrease in scale length and width observed in some taxa led to changes in the scale size while conserving its overall shape (e.g., *M. bronchartiana*, *M. elevate*, *M. pumilio* var. *dispersa*), whereas disproportional changes in scale length and width resulted in the origin of new scale shape in other species (e.g., *M. asmundiae*, *M. corymbosa*, *M. torquata*; Fig. 5).

DISCUSSION

Molecular phylogeny of the genus Mallomonas. The timing of major diversification events in our time-calibrated phylogenetic analysis is closer to the latest analysis presented by Siver et al. (2015) than to the analysis presented by Jo et al. (2013), although our estimated diversifications of taxa are slightly younger. Similarly, the topology and relationships of *Mallomonas* species are largely congruent with the phylogeny presented in Siver et al. (2015) with several minor changes. With high statistical support, *M. adamas* is sister to clade comprising of *M. punctifera*, *M. splendens*, and *M. bronchartiana*. Contrastly, in Siver et al. (2015), *M. adamas* was sister to clade comprising of *M. splendens*, and *M. bronchartiana*. Further, *M. matvienkoae* is sister to *M. pseudomatvienkoae*, not sister to clade comprising taxa *M. pseudomativenkoae*, *M. hexareticulata*, and *M. sorohexareticulata*. In our phylogeny, *M. elevata* is sister to *M. mangofera* f. *foveata*, not to *M. torquata*. Also, *M. annulata* is sister to all taxa from the sections *Papillosae*, *Akrokomae*, *Striatae*, *Pseudocoronatae*, *Mallomonas*, and *Leboimeanae*, not only to *M. akrokomos*. In the phylogeny presented by Siver et al. (2015), *M. areolata* is sister to many taxa from the section *Mallomonas*, while in the phylogeny presented here, *M. areolata* is sister to clade comprising of *M. elongata* and *M. alpina* (also from the section *Mallomonas*). Lastly, *M. morrisonensis* is sister to *M. muskokana*, not sister to clade comprising of taxa *M. muskokana*, *M. crassisquana*, and *M. acaroides*.

The two newly sequenced taxa, *Mallomonas intermedia* and *M. pumilio* var. *dispersa*, were placed into sections *Mallomonas* and *Torquatae*, respectively, where they morphologically belong to. The taxa *M. intermedia* is closely related to *M. portae-ferreae* with similar phenotype, though scales of the latter have more complex morphology. The taxa *M. pumilio* var. *dispersa* is sister to *M. torquata*, also possessing very similar morphology of scales. However, the third newly sequenced taxa, *M. paludosa*, was placed in the section *Mallomonas*, even though

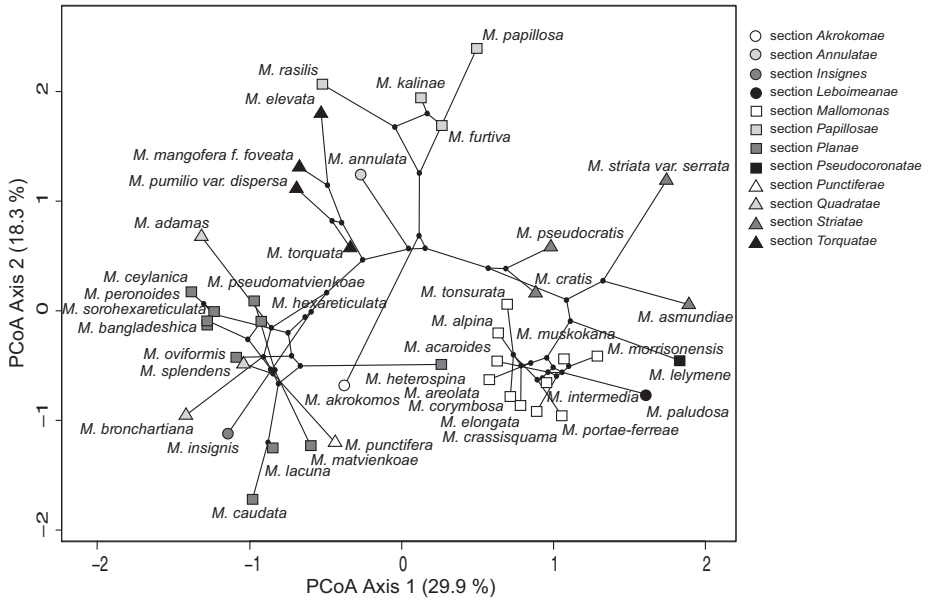

FIG. 3. A principle coordinate analysis (PCoA) of *Mallomonas* phenotypes based on 29 morphological characters scored on silica scales and cases. The phylogenetic relationships among species were projected into the ordination diagram, forming a "phylomorphospace plot." The nodes are depicted as black dots, their position reflecting the reconstructed ancestral phenotypes. Species are color-coded following the classification of the genus into particular sections.

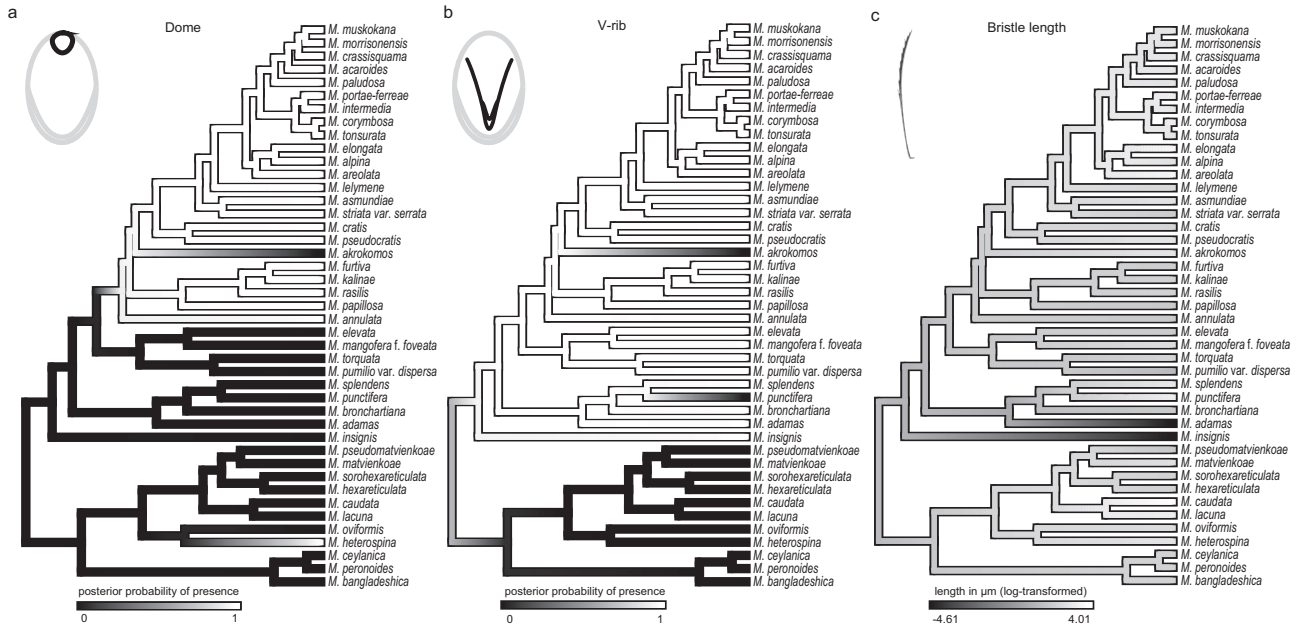

FIG. 4. Ancestral character reconstructions showing the evolution of three traits in the genus *Mallomonas*: dome (a), V-rib (b), and bristle length (c).

it is morphologically characterized as a member of the section *Leboimeanae*. Thus, we suggest a reclassification of *M. paludosa* (possibly also other members of the section *Leboimeanae*) and their inclusion in the section *Mallomonas*. Likewise, in line with the previous studies (e.g., Jo et al. 2013, Kim et al. 2014, Siver et al. 2015), we show that the section *Striatae* is not monophyletic.

The differences between our phylogeny and phylogeny presented in Siver et al. (2015) could be attributed to different number of used molecular markers (three in this study compared with five in Siver et al. 2015) and to each species being represented by a single strain in our study (compared with multiple strains in Siver et al. 2015). Nonetheless, the topologies are highly congruent, which supports using our phylogeny to reconstruct the evolution of morphological traits.

The evolution of phenotype from Mallomonas *ancestor to modern taxa.* According to trait evolution reconstructions, scales of the common ancestor were likely equipped with papillae on the shield and perforations (pores) on both shield and posterior flange. The ancestral scales could be even more complex because our analyses only account for traits present in the modern taxa with available sequence data. While bristles were probably present in the common ancestor of the *Mallomonas* genus, it is not clear whether a common ancestor of A1 subclade still had bristles. This is because the most ancient lineages of A1 subclade lack bristles completely and many of the later divided taxa possess bristles only on anterior and/or posterior ends of the silica case (Fig. S1). However, we did not consider different types of bristles, that is, with a solid shaft versus with a rolled shaft (Siver et al. 2015) since this information is not available for all species. In fact, these additional data may have given us more information about the bristle origin. Interestingly, the most ancient lineages within the sister genus *Synura* (e.g., *S. uvella*, *S. splendida*) also possess silica projections from their scales, called spines, and we could speculate that these structures might have originated from the same ancestral precursor as *Mallomonas* bristles.

One of the earliest events that happened in the *Mallomonas* evolution was the formation of the V-rib. This structure evolved either in the common ancestor of the genus or early in the A1 subclade after the A1 and A2 subclades split (approximately at 113 Ma; Fig. 4b). Lineages A1 and A2 are defined by the presence or absence of the V-rib, respectively (Siver et al. 2015). However, there are two species lacking the V-rib in spite of their phylogenetic position within the A1 subclade (i.e., *M. punctifera* and *M. akrokomos*). Interestingly, this was not mentioned in any of the previous molecular studies (Jo et al. 2011, 2013, Kim et al. 2014, Siver et al. 2015) and information about the V-rib is also missing in the original descriptions of these species (Korshikov 1941, Harris 1958, Kristiansen and Preisig 2007). Nonetheless, we can still recognize its presumable rudiments, the indistinct longitudinal ribs of *M. akrokomos* and the pronounced anterior submarginal ribs of *M. punctifera*. Another conspicuous structure, the dome, emerged further in the *Mallomonas* evolution. The dome appeared on body scales of the A1 representatives at 70 Ma (Fig. 4a);

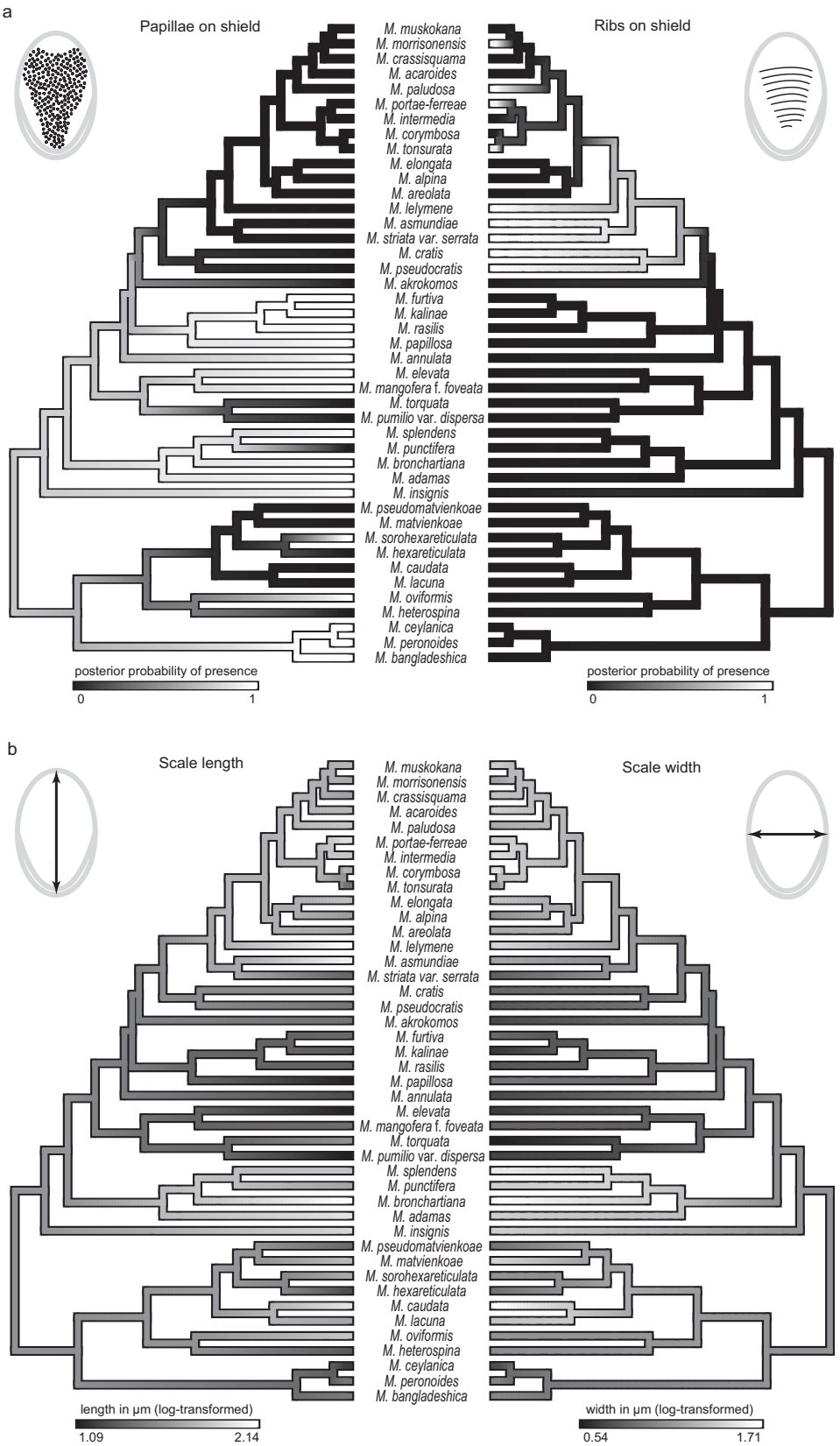

FIG. 5. Pairwise comparisons of reconstructed evolution for two binary (a) and two quantitative (b) morphological traits in the genus *Mallomonas* provided by ancestral character reconstructions.

however, it is very likely it was already present on apical and caudal scales long before. This is linked with its function in bristle attachment through a part called the foot that is tucked under the dome. As described above, in the most ancient A1 taxa, bristles are either absent or restricted to ends of the silica case. Therefore domes were most likely present on apical and/or caudal scales, which are placed at anterior and posterior ends on cells, respectively, as we can see in several contemporary taxa (e.g., *M. elevata*, *M. mangofera* f. *foveata*, *M. torquata*, *M. pumilio* var. *dispersa*, *M. splendens*). The dome also secondarily disappeared from body scales of *M. akrokomos*, even though it is still present on their apical scales. Interestingly, a different way of bristle attachment originated in the A2 lineage, where a flat foot of the bristle is simply tucked under the proximal end of the scale. There is no dome on any type of scale among the A2 taxa, with the only exception of *M. heterospina*. Despite the similar appearance and function in bristle attachment, the dome of *M. heterospina* is not homologous to the dome in the A1 subclade. This structure originated independently and should be treated as a dome-like structure (Fig. S3 in the Supporting Information).

Both the dome and the V-rib are extremely conservative structures with only rare cases of their evolutionary loss. This is most likely due to structural and/or developmental constraints, such as bristle attachment and their key role in organizing scales into a compact silica case, for the dome and the V-rib, respectively (Siver and Glew 1990, Siver 1991). An alternative way of creating a compact silica case is by production of larger and rather plain scales that overlap to a great extent. This latter scenario is apparent in many A2 lineage taxa (e.g., *Mallomonas caudata* and *M. hexareticulata*).

Interestingly, the bristles gradually increase in size during the *Mallomonas* genus evolution.

Taking into account the oscillations in climatic conditions occurring over the last 150 Ma, it is unlikely that unidirectional change in bristle length could have been triggered by a climate change. Instead, this might have been a consequence of selection to escape predation. Longer spines and bristles could prevent predator attacks (Raven and Giordano 2009, Finkel and Kotrc 2010, van Tol et al. 2012). These structures could also slow sinking from upper water layers (Padisák et al. 2003), though the flagellated cells of *Mallomonas* are capable of active movement.

There are also traits that were inherited in unchanged form for more than 50 million years and from the *Mallomonas* evolution perspective, we can classify them as medium dynamic. This concerns pores on shield, pores on posterior flange, window, mesh on posterior flange and U-shaped ridge (Fig. S1). These perforations and structural reinforcements probably represent constraints of a scale construction and are evolutionarily conserved.

On the other hand, ribs on the shield are one of the most recently evolved structures (Fig. 5a). Interestingly, morphologically similar ribs on the posterior flange in *Mallomonas insignis* and *M. heterospina* evolved independently. The ribs on the shield originated in the Paleocene, approximately at 60 Ma, which was a time of substantial global environmental changes, such as increase in temperature and cosmic radiation (e.g., Shaviv 2003, Gingerich 2006). It is possible that the formation of ribs was a response to these environmental changes (e.g., by shielding off the UV-B radiation more efficiently and thus preventing cell damage). Similarly, an increase in efficiency of UV-B protection due to surface structuring of silica cases was previously demonstrated in modern diatoms (Ellegaard et al. 2016).

Some traits did not last in unchanged form for more than 25 million years. Most of these highly dynamic traits are connected to size and shape of scale and silica case (scale and cell case length and width and scale roundness). This could be linked with a need to quickly change the scale or case size. As Siver et al. (2015) suggested, a change in scale size could follow a change in temperature. According to the temperature-size rule in protists, their cells linearly decrease in size with an increase in temperature (Montagnes and Franklin 2001, Atkinson et al. 2003). To optimize a precise cell coverage by the silica case, a decrease in cell size should be followed by the decrease in scale size. Such ability to readily modify the cell and scale size could be the key aspect in the evolutionary success of *Mallomonas* taxa. This is evident when comparing the fossil and contemporary scales of *M. insignis* that persisted in an almost unchanged form over the last 40 million years except their apparent size reduction (Siver and Wolfe 2009, Siver et al. 2013b). Similar morphological stasis concerns also the species *M. asmundiae*, *M. bangladeshica*, *M. lychenensis*, *M. multiunca*, and *M. peronoides*.

On the other hand, the overall phenotype was rapidly changed within the last 25 million years in *Mallomonas ceylanica*, *M. corymbosa*, *M. morrisonensis*, *M. portae-ferreae*, and *M. tonsurata* (see Fig. 5, Figs. S1 and S2).

Morphological similarity of *Mallomonas* species generally reflects their phylogenetic relationships. Therefore, the traditional species concept based on silica scale morphology seems to be justified for a basic classification of species into the particular sections. However, in some cases the morphological data alone are not suitable for estimating species classification since some differ greatly in their morphology from their closest relatives (see species of the *Planae* and *Quadratae* sections in the phylomorphospace plot, Fig. 3).

In this study, the species morphology was evaluated mainly based on silica scales. For this evaluation, multiple microphotographs and in a few cases only a single microphotograph were used per species. The majority of microphotographs was taken using TEM; however, for some species there are only SEM microphotographs available. Moreover, several analyzed microphotographs had rather poor image resolution. Theoretically, the morphological evaluations could have been also influenced by intraspecific morphological variation of individuals due to phenotypic plasticity, particularly in cases when limited number of strains was available per species. These shortcomings might have especially influenced the evaluations of *Mallomonas hexareticulata*, *M. lacuna*, *M. pseudomatvienkoae*, *M. sorohexareticulata*, and *M. splendens*. Despite this, the overall strong correlation of phenotypic similarity and genetic relatedness suggests that morphological evaluations conducted in this study had sufficient power to describe species' phenotypes.

Most importantly, the evolution of phenotype was reconstructed on the basis of only a quarter of described *Mallomonas* species. Due to this, it is possible that we did not detect all evolutionary trends. In addition, the structures that originated only once based on the results of our study could, in fact, have originated multiple times. However, the molecular data for the other members of the genus *Mallomonas* are lacking, which is mainly due to general difficulties with their cultivation. In the future, the cultivation difficulties could be solved by meta-barcoding studies applying next-generation sequencing techniques; however, these data sets would be affected by the complete lack of morphological data. Nonetheless, all the *Mallomonas* representatives with molecular data available were included in our study and we also obtained the molecular data for three more taxa. It is worth mentioning that in our study we omitted the taxon "*Mallomonas sorofavus*" reported in Kim et al. 2014 as this is not a valid species name. According to molecular data supplied by the authors (strain Gungnam092709, GenBank accession numbers: JN991183, JN991192, JN991174) the investigated strain in fact belong to *M. sorohexareticulata*.

We thank Katherine Drotos and two anonymous reviewers for their very helpful comments. We are also grateful to Martin Pusztai for help with sample collection and Jana Kulichová for providing us with a microphotograph of *Mallomonas heterospina*. The study was supported by the Charles University (GAUK, project no. 1304317). Additional support was provided by the Czech Academy of Sciences (long-term research development project no. RVO 67985939).

Andersen, R. A. 2007. Molecular systematics of the Chrysophyceae and Synurophyceae. *In* Brodie, J. & Lewis, J. [Eds.] *Unravelling the Algae*. CRC Press, New York, pp. 285–313.

Andersen, R. A., Morton, S. L. & Sexton, J. P. 1997. Provasoli-Guillard National Center for culture of marine phytolankton 1997 list of strains. *J. Phycol.* 33:1–75.

Asmund, B. & Kristiansen, J. 1986. The genus *Mallomonas* (Chrysophyceae). *Opera Bot.* 85:5–128.

Atkinson, D., Ciotti, B. J. & Montagnes, D. J. S. 2003. Protists decrease in size linearly with temperature: ca. 2.5% C-1. *Proc. R. Soc. B Biol. Sci.* 270:2605–11.

Bovee, E. C. 1981. Distribution and forms of siliceous structures among Protozoa. *In* Simson, T. L. & Volcani, B. E. [Eds.] *Silicon and Siliceous Structures in Biological Systems*. Springer, New York, pp. 233–79.

Brakefield, P. M. & Roskam, J. C. 2006. Exploring evolutionary constraints is a task for an integrative evolutionary biology. *Am. Nat.* 168(Suppl):S4–13.

Creaser, R. A., Grütter, H., Carlson, J. & Crawford, B. 2004. Macrocrystal phlogopite Rb–Sr dates for the Ekati property kimberlites, Slave Province, Canada: evidence for multiple intrusive episodes in the Paleocene and Eocene. *Lithos* 76:399–414.

Darriba, D., Taboada, G. L., Doallo, R. & Posada, D. 2012. jModelTest 2: more models, new heuristics and parallel computing. *Nat. Methods* 9:772.

Darwin, C. 1859. *On the Origin of Species by Means of Natural Selection, or the Preservation of Favoured Races in the Struggle for Life*. Nature, London, 502 pp.

Daugbjerg, N. & Andersen, R. A. 1997. Phylogenetic analyses of *rbc*L sequences from haptophytes and heterokont algae suggest their chloroplasts are unrelated. *Mol. Biol. Evol.* 14:1242–51.

Doria, G., Royer, D. L., Wolfe, A. P., Fox, A., Westgate, J. A. & Beerling, D. J. 2011. Declining atmospheric CO_2 during the late Middle Eocene climate transition. *Am. J. Sci.* 311:63–75.

Drummond, A. J. & Rambaut, A. 2007. BEAST: Bayesian evolutionary analysis by sampling trees. *BMC Evol. Biol.* 7:214.

Eldredge, N. & Gould, S. J. 1972. Punctuated equilibria: an alternative to phyletic gradualism. *In* Schopf, T. J. M. [Ed.] *Models in Paleobiology*. Freeman-Cooper, San Francisco, California, pp. 82–115.

Eldredge, N. & Gould, S. J. 1996. *Fossils: The Evolution and Extinction of Species*. Princeton University Press, Princeton, New Jersey, 240 pp.

Ellegaard, M., Lenau, T., Lundholm, N., Maibohm, C., Friis, S. M. M., Rottwitt, K. & Su, Y. 2016. The fascinating diatom frustule—can it play a role for attenuation of UV radiation? *J. Appl. Phycol.* 28:3295–306.

Erwin, D. H. 2000. Macroevolution is more than repeated rounds of microevolution. *Evol. Dev.* 2:78–84.

Felsenstein, J. 1985. Phylogenies and the comparative method. *Am. Nat.* 125:1.

Finkel, Z. V. & Kotrc, B. 2010. Silica use through time: macroevolutionary change in the morphology of the diatom fustule. *Geomicrobiol J.* 27:596–608.

Fritz, S. A. & Purvis, A. 2010. Selectivity in mammalian extinction risk and threat types: a new measure of phylogenetic signal strength in binary traits. *Conserv. Biol.* 24:1042–51.

Gersick, C. J. G. 1991. Revolutionary change theories: a multilevel exploration of the punctuated equilibrium paradigm. *Acad. Manag. Rev.* 16:10.

Gingerich, P. D. 2006. Environment and evolution through the Paleocene-Eocene thermal maximum. *Trends Ecol. Evol.* 21:246–53.

Gould, S. J. 2002. *The Structure of Evolutionary Theory*. Harvard University Press, Cambridge, Massachusetts, 1433 pp.

Harris, K. 1958. A Study of *Mallomonas insignis* and *Mallomonas akrokomos*. *J. Gen. Microbiol.* 19:55–64.

Henriksen, P., Knipschildt, F., Moestrup, Ø. & Thomsen, H. A. 1993. Autecology, life history and toxicology of the silicoflagellate *Dictyocha speculum* (Silicoflagellata, Dictyochophyceae). *Phycologia* 32:29–39.

Jo, B. Y., Shin, W., Boo, S. M., Kim, H. S. & Siver, P. A. 2011. Studies on ultrastructure and three-gene phylogeny of the genus *Mallomonas* (Synurophyceae). *J. Phycol.* 47:415–25.

Jo, B. Y., Shin, W., Kim, H. S., Siver, P. A. & Andersen, R. A. 2013. Phylogeny of the genus *Mallomonas* (Synurophyceae) and descriptions of five new species on the basis of morphological evidence. *Phycologia* 52:266–78.

Katana, A., Kwiatowski, J., Spalik, K., Zakrys, B., Szalacha, E. & Szymanska, H. 2001. Phylogenetic position of *Koliella* (Chlorophyta) as inferred from nuclear and chloroplast small subunit rDNA. *J. Phycol.* 37:443–51.

Katoh, K. & Standley, D. M. 2013. MAFFT multiple sequence alignment software version 7: improvements in performance and usability. *Mol. Biol. Evol.* 30:772–80.

Kim, H. S., Kim, J. H., Shin, W. & Jo, B. Y. 2014. *Mallomonas elevata* sp. nov. (Synurophyceae), a new scaled Chrysophyte from Jeju Island, South Korea. *Nov. Hedwigia.* 98:89–102.

Korshikov, A. A. 1941. On some new or little known flagellates. *Arch. für Protistenkd.* 95:22–44.

Kristiansen, J. 2002. The genus *Mallomonas* (Synurophyceae) - A taxonomic survay based on the ultrastructure of silica scales and bristles. *Opera Bot.* 139:5–218.

Kristiansen, J. 2005. *Golden Algae: A Biology of Chrysophyta.* Gantner Verlag, Germany, 167 pp.

Kristiansen, J. & Preisig, H. R. 2007. *Süßwasserflora von Mitteleuropa Freswater Flora of Central Europe: Chrysophyte and Haptophyte Algae*, 2nd edn. Springer, Berlin, 252 pp.

Lavau, S., Sounders, G. W. & Wetherbee, R. 1997. A phylogenetic analysis of the Synurophyceaea using molecular data and scale case morphology. *J. Phycol.* 33:135–51.

Lavau, S. & Wetherbee, R. 1994. Structure and development of the scale case of *Mallomonas adamas* (Synurophyceae). *Protoplasma* 181:259–68.

Lepš, J. & Šmilauer, P. 2014. *Multivariate Analysis of Ecological Data Using CANOCO 5.2.* Cambridge University Press, Cambridge, Massachusetts, 373 pp.

Martin-Jezequel, V., Hildebrand, M. & Brzezinski, M. A. 2000. Silicon metabolism in diatoms: implications for growth. *J. Phycol.* 36:821–40.

Mayama, S. & Kuriyama, A. 2002. Diversity of mineral cell coverings and their formation processes: a review focused on the siliceous cell coverings. *J. Plant. Res.* 115:289–95.

Montagnes, D. & Franklin, D. 2001. Effect of temperature on diatom volume, growth rate, and carbon and nitrogen content: reconsidering some paradigms. *Limnol. Oceanogr.* 46:2008–18.

Morais, L., Fairchild, T. R., Lahr, D. J. G., Rudnitzki, I. D., Schopf, J. W., Garcia, A. K., Kudryavtsev, A. B. & Romero, G. R. 2017. Carbonaceous and siliceous Neoproterozoic vase-shaped microfossils (Urucum Formation, Brazil) and the question of early protistan biomineralization. *J. Paleontol.* 91:393–406.

Nei, M. 2005. Selectionism and neutralism in molecular evolution. *Mol. Biol. Evol.* 22:2318–42.

Orr, H. A. 2005. The genetic theory of adaptation: a brief history. *Nat. Rev. Genet.* 6:119–27.

Padisák, J., Soróczki-Pintér, É. & Rezner, Z. 2003. Sinking properties of some phytoplankton shapes and the relation of form resistance to morphological diversity of plankton – an experimental study. *Hydrobiologia* 500:243–57.

Pagel, M. 1999. Inferring the historical patterns of biological evolution. *Nature* 401:877–84.

Popescu, A. A., Huber, K. T. & Paradis, E. 2012. ape 3.0: new tools for distance-based phylogenetics and evolutionary analysis in R. *Bioinformatics* 28:1536–7.

Pusztai, M., Čertnerová, D., Škaloudová, M. & Škaloud, P. 2016. Elucidating the phylogeny and taxonomic position of the genus *Chrysodidymus* Prowse (Chrysophyceae, Synurales). *Cryptogam. Algol.* 37:297–307.

R Development Core Team. 2017. *R: A Language and Environment for Statistical Computing.* R Foundation for Statistical Computing, Vienna, Austria.

Rambaut, A. 2009. FigTree version 1.3.1. Available at http://tree.bio.ed.ac.uk (last accessed 28 October 2018).

Raven, J. A. & Giordano, M. 2009. Biomineralization by photosynthetic organisms: evidence of coevolution of the organisms and their environment? *Geobiology* 7:140–54.

Revell, L. J. 2012. Phytools: an R package for phylogenetic comparative biology (and other things). *Methods. Ecol. Evol.* 3:217–23.

Revell, L. J. 2013. Two new graphical methods for mapping trait evolution on phylogenies. *Methods Ecol. Evol.* 4:754–9.

Roger, A. J. & Hug, L. A. 2006. The origin and diversification of eukaryotes: problems with molecular phylogenetics and molecular clock estimation. *Philos. Trans. R. Soc. B Biol. Sci.* 361:1039–54.

Schluter, D., Price, T., Mooers, A. O. & Ludwig, D. 1997. Likelihood of ancestor states in adaptive radiation. *Evolution* 51:1699.

Schneider, C. A., Rasband, W. S. & Eliceiri, K. W. 2012. NIH Image to ImageJ: 25 years of image analysis. *Nat. Meth.* 9:671–5.

Shaviv, N. J. 2003. The spiral structure of the Milky Way, cosmic rays, and ice age epochs on Earth. *New Astron.* 8:39–77.

Siver, P. A. 1991. *The Biology of Mallomonas: Morphology, Taxonomy and Ecology.* Kluwer Academic Publisher, Dordrecht, 230 pp.

Siver, P. A. 2013. Variability in scale shape between ancient and modern specimens of *Mallomonas insignis*. *Nov. Hedwigia.* 142:127–39.

Siver, P. A. & Glew, J. R. 1990. The arrangement of scales and bristles on *Mallomonas* (Chrysophyceae): a proposed mechanism for the formation of the cell covering. *Can. J. Bot.* 68:374–80.

Siver, P. A., Jo, B. Y., Kim, J. I., Shin, W., Lott, A. M. & Wolfe, A. P. 2015. Assessing the evolutionary history of the class Synurophyceae (Heterokonta) using molecular, morphometric, and paleobiological approaches. *Am. J. Bot.* 102:921–41.

Siver, P. A., Lott, A. M. & Wolfe, A. P. 2013a. A summary of *Synura* taxa in early Cenozoic deposits from Northern Canada. *Nov. Hedwigia.* 142:181–90.

Siver, P. A. & Wolfe, A. P. 2005. Eocene scaled chrysophytes with pronounced modern affinities. *Int. J. Plant Sci.* 166:533–6.

Siver, P. A. & Wolfe, A. P. 2009. Tropical ochrophyte algae from the eocene of northern Canada: a biogeographic response to past global warming. *Palaios* 24:192–8.

Siver, P. A., Wolfe, A. P., Rohlf, F. J., Shin, W. & Jo, B. Y. 2013b. Combining geometric morphometrics, molecular phylogeny and micropalaeontology to assess evolutionary patterns in *Mallomonas* (Synurophyceae: Heterokontophyta). *Geobiology* 11:127–38.

Škaloud, P., Kristiansen, J. & Škaloudová, M. 2013a. Developments in the taxonomy of silica-scaled chrysophytes - From morphological and ultrastructural to molecular approaches. *Nord. J. Bot.* 31:385–402.

Škaloud, P., Škaloudová, M., Pichrtová, M., Němcová, Y., Kreidlová, J. & Pusztai, M. 2013b. www.chrysophytes.eu - a database on distribution and ecology of silica-scaled chrysophytes in Europe. *Nov. Hedwigia* 142:141–6.

Swofford, D. L. 2001. *PAUP*. Phylogenetic Analysis Using Parsimony (* and Other Methods), Version 4.* Sinauer Associates, Sunderland, Massachusetts.

Tamura, K., Peterson, D., Peterson, N., Stecher, G., Nei, M. & Kumar, S. 2011. MEGA5: molecular evolutionary genetics analysis using maximum likelihood, evolutionary distance, and maximum parsimony methods. *Mol. Biol. Evol.* 28:2731–9.

van Tol, H. M., Irwin, A. J. & Finkel, Z. V. 2012. Macroevolutionary trends in silicoflagellate skeletal morphology: the costs and benefits of silicification. *Paleobiology* 38:391–402.

Untergasser, A., Cutcutache, I., Koressaar, T., Ye, J., Faircloth, B. C., Remm, M. & Rozen, S. G. 2012. Primer3–new capabilities and interfaces. *Nucleic Acids Res.* 40:e115.

Wolfe, A. P. & Siver, P. A. 2013. A hypothesis linking chrysophyte microfossils to lake carbon dynamics on ecological and evolutionary time scales. *Glob. Planet. Change* 111:189–98.

Zwickl, D. J. 2006. Genetic algorithm approaches for the phylogenetic analysis of large biological sequence datasets under the maximum likelihood criterion. PhD thesis, The University of Texas, Austin, 115 pp.

Supporting Information

Additional Supporting Information may be found in the online version of this article at the publisher's web site:

Figure S1. Ancestral character reconstructions showing the evolution of 15 binary morphological traits in the genus *Mallomonas*.

Figure S2. Ancestral character reconstructions showing the evolution of seven quantitative morphological traits in the genus *Mallomonas*.

Figure S3. TEM microphotographs illustrating how bristles are attached to scales either through dome-like structure (a) in *Mallomonas heterospina* and dome (b) in *M. papillosa*.

Table S1. Collection details for the strains of Chrysophyceae used in this study and GenBank accession numbers for the respective nr SSU, nr LSU, and *rbc*L gene sequences.

Table S2. Values of 29 morphological traits scored on 43 representatives of the genus *Mallomonas*.

Table S3. Values of two parameters describing the strength of phylogenetic influence on the evolution of particular morphological traits. The parameter D was estimated for binary traits (a), and the parameter λ (lambda) was estimated for quantitative traits (b). For both parameters, statistical tests were conducted to assess whether the parameter values are equal to 0 (i.e., no effect of phylogeny on trait evolution) or 1 (i.e., trait evolution can be explained entirely by phylogenetic relationships among taxa).